Simulating Induced Interdigitation in Membranes

Marieke Kranenburg, Martin Vlaar, and Berend Smit

Department of Chemical Engineering, University of Amsterdam, Amsterdam, The Netherlands

ABSTRACT   In this study we introduce a mesoscopic lipid-water-alcohol model. Dissipative particle dynamics (DPD) simulations have been used to investigate the induced interdigitation of bilayers consisting of double-tail lipids by adding alcohol molecules to the bilayer. Our simulations nicely reproduce the experimental phase diagrams. We find that alcohol can induce an interdigitated structure where the common bilayer structure changes into monolayer in which the alcohol molecules screen the hydrophobic tails from the water phase. At low concentrations of alcohol the membrane has domains of the interdigitated phase that are in coexistence with the common membrane phase. We compute the effect of the chain length of the alcohol on the phase behavior of the membrane and show that the stability of the interdigitated phase depends on the length of the alcohol. We show that we can reproduce the experimental hydrophobic thickness of the bilayer for various combinations of lipids and alcohols. We use our model to clarify some of the experimental questions related to the structure of the interdigitated phase and put forward a simple model that explains the alcohol chain length dependence of the stability of this interdigitated phase.

INTRODUCTION

Adsorption of alcohol molecules or other small amphiphilic molecules in the cell membrane can induce significant changes in the structure of the membrane. These structural changes of the membrane can influence the conformation of proteins or other structures embedded in the membrane. Experiments on phospholipid membranes have shown that alcohol can, for example, induce the interdigitated phase (Slater and Huang, 1988). This is an extreme example of the effect alcohol can have on the structure of a membrane. In an ordinary membrane the hydrophobic thickness is approximately twice the length of the hydrophobic tails of a phospholipid, in the interdigitated phase the hydrophobic thickness is reduced to the sum of the length of the hydrophobic tails of a single phospholipid and the alcohol. Understanding these induced structural changes is therefore not only of fundamental interest but might also give us a better understanding of the functioning of cell membranes.

Various factors have been identified to induce interdigitation (Slater and Huang, 1988). Besides adding small amphiphilic molecules, like anesthetics (Hata et al., 2000) or alcohol, other factors are changes in the environment, like in the changes in the hydrostatic pressure or in the pH of the solution (Furuike et al., 1999) or changes in the molecular structure of the lipid—for example by introducing an ester-linkage in the headgroup of the phospholipids (Lewis et al., 2001; Winter et al., 2001). In this work we focus on the effect of adding small amphiphilic molecules. Short-chain alcohols (methanol through heptanol) are known to induce interdigitation (Rowe, 1983; McIntosh et al., 1983, 2001; Adachi

et al., 1995; Simon and McIntosh, 1984). In the first instance it was found that these alcohols have two different effects on the transition from the low temperature gel phase to the high temperature fluid phase, dependent on concentration (Rowe, 1983). At low concentrations of alcohol, the main transition temperature shifts to a lower temperature, whereas at high concentrations this transition temperature shifts to a higher temperature compared to a pure lipid bilayer. This effect was called the ''biphasic effect.'' Subsequently, Simon and McIntosh (1984) observed in their study the formation of the interdigitated phase at high concentrations of alcohol, which explains the biphasic effect. At low concentrations of alcohol the disorder of the lipid tails increases, leading to a lower transition temperature. At high concentrations the more tightly packed interdigitated phase is formed, resulting in an increase of the transition temperature.

Interdigitation can be understood if we consider the location of the alcohol molecules in the bilayer. The alcohol molecules replace the interfacial water molecules: the OH group binds to the phosphate group of the lipid headgroup and the hydrophobic tail sticks into the hydrophobic core of the bilayer. Since the OH-group binds to the phosphate moiety of the lipid headgroup (Chiou et al., 1992), lateral space is created between the headgroups, leading to voids in the hydrophobic core. These voids are energetically unfavorable and thus the system will minimize the energy by the formation of an interdigitated phase. By interdigitation the system gains energy due to the stronger van der Waals interaction in the interdigitated phase compared to the noninterdigitated phase (Simon and McIntosh, 1984; Ohki et al., 1990; Feller et al., 2002) and due to an entropy gain by replacing the highly ordered water molecules at the interface by alcohol molecules (Simon and McIntosh, 1984; Rowe and Campion, 1994; McIntosh et al., 2001). Since the tail ends of the alcohol molecules shield the tail ends of the lipids

from the interfacial water, the energy cost in the formation of the interdigitated phase is minimized.

Phase diagrams of various lipids and alcohols are constructed (Nambi et al., 1988; Ohki et al., 1990; Vierl et al., 1994; Löbbecke and Cevc, 1995; see also this article, Fig. 1, for a schematic sketch of an experimental phase diagram). At high temperatures the fluid L_α phase is stable. At low temperatures, various structures are found, dependent on temperature and alcohol concentration. At low concentrations, we find the transition from the highly ordered subgel or L_c phase via the gel phase $L_{\beta'}$ to the rippled phase $P_{\beta'}$. In all these phases the tails have a tilt with respect to the bilayer normal. At high concentrations of alcohol the rippled phase disappears, and the interdigitated phase $L_{\beta I}$ is formed, in which the tails do not show a tilt. In between these extremes a coexistence region is observed between the rippled phase or the gel phase and the interdigitated phase.

The addition of alcohol has a larger effect on the pretransition $L_{\beta'} \to P_{\beta'}$ than on the main transition $P_{\beta'} \to L_\alpha$. At low concentrations of alcohol this transition is shifted to lower temperatures and after the critical concentration $c_{L_{\beta I}}$ (the concentration at which interdigitation is complete) the rippled phase disappears (Veiro et al., 1987). Questions in the formation of the interdigitated phase which are still not (completely) solved are the distribution of the alcohols in the bilayer, the exact molecular structure of the alcohol-induced interdigitated phase, and the concentration of alcohol in the lipid bilayer at which interdigitation occurs.

These experimental uncertainties motivated us to use molecular simulation to study the effect of alcohol. State-of-

the-art molecular dynamics simulations give detailed structural information on the position of alcohol molecules in a lipid bilayer (Koubi et al., 2003; Tang and Xu, 2002), but are too time-consuming to observe structural changes in the membrane. As an alternative we use a hierarchical approach in which realistic all-atom simulations are used to determine the effective interaction parameters of a mesoscopic model. At this mesoscopic level simulations are 4–5 orders-of-magnitude more efficient (Groot and Rabone, 2001; Shelley et al., 2001), allowing us to compute complete phase diagrams. Whereas previous mesoscopic simulations were aimed at qualitative insights, here we demonstrate that such a hierarchical mesoscopic model yields semiquantitative predictions of the structure of a membrane. In Kranenburg et al. (2003a,b) we showed that a bilayer, consisting of monotail lipids, can spontaneously form the interdigitated $L_{\beta I}$ phase. Interdigitation does not occur in bilayers of symmetrical chain phospholipids, but has to be induced by attaching an additional group to the head of a double tail lipid. To understand the molecular mechanisms underlying the formation of the interdigitated phase, we extend our mesoscopic model to study the effect of alcohol on the structure of a membrane. Experimentally it is very difficult to measure the concentration of alcohol in the membrane directly. Thus, the main advantage of our mesoscopic approach aimed at such a system is that we can directly determine the mole fraction of alcohol molecules needed to induce a fully interdigitated phase.

Model and computational details

In our lipid-water-alcohol model, we distinguish three types of particles, w, h, and t, to mimic water and the head- and tail-atoms of a lipid, respectively. The hydrophilic and hydrophobic particles interact via a soft-repulsion model commonly used in dissipative particle dynamics (DPD) (Groot and Warren, 1997; Frenkel and Smit, 2002). In a DPD simulation a particle represents the center of mass of a cluster of atoms. The total force on such a particle consists of dissipative, random, and conservative forces. The dissipative and random forces are chosen such that a proper canonical distribution is sampled (Frenkel and Smit, 2002). For the conservative force we use the conventional soft-repulsive interaction, given by

$$F_{ij}^C = \begin{cases} a_{ij}(1 - r_{ij}) & r_{ij} < r_c, \\ 0 & r_{ij} \geq r_c, \end{cases} \quad (1)$$

where r_{ij} is the distance between particles i and j, a_{ij} is the parameter characterizing the interaction between two particles, and r_c is the cutoff radius. The DPD parameters are related to the compressibility of water and to Flory-Huggins solubility parameters such that a reasonable description of the thermodynamics of the real system can be obtained (Groot and Warren, 1997).
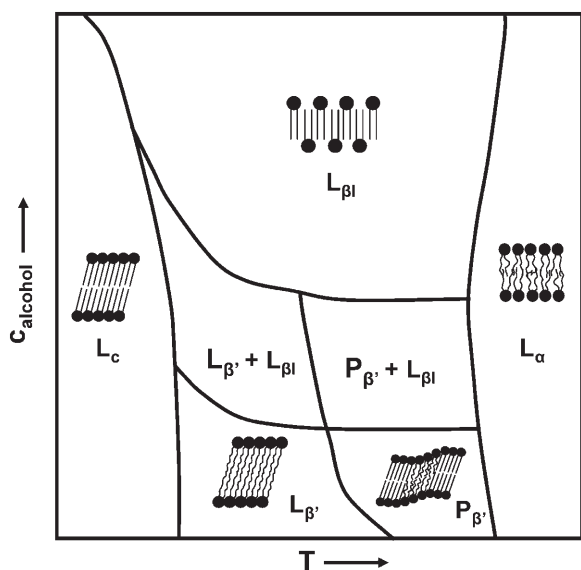

FIGURE 1   Schematic representation of the phase diagram of a phosphatidylcholine/alcohol mixture as a function of alcohol concentration and temperature (Nambi et al., 1988; Ohki et al., 1990; Vierl et al., 1994; Löbbecke and Cevc, 1995). The various phases are schematically drawn and are explained in the text.

We consider lipids consisting of a headgroup with three hydrophilic segments and two tails with variable length (see Fig. 2), which mimics phospholipid distearoyl-phosphatidylcholine (DSPC). We assume that a DPD particle occupies a volume of 90 Å^3, which results in a mapping in which DSPC is represented by three hydrophilic head beads and two 7-bead tails ($h_3(t_7)_2$). For a correct description of the experimental chain length dependence of the area per lipid, it is essential to properly reproduce the conformations of the lipid. Molecular dynamics simulations of a single phospholipid in water using a realistic all-atom representation are used to generate configurations of the lipid, which were subsequently used to optimize the intramolecular interactions (bond-bending and bond-vibration) of the DPD model (Kranenburg et al., 2004b). We used similar parameters to Groot and Warren (1997) for the soft-repulsions in the conservative DPD interactions ($a_{ww} = a_{tt} = 25$, $a_{ht} = a_{wt} = 80$, $a_{hh} = 35$, and $a_{hw} = 15$); the intramolecular interactions include a bond-bending potential,

$$U_\theta = (1/2)k_\theta(\theta - \theta_0)^2, \quad (2)$$

with $k_\theta = 6$ and $\theta_0 = 180°$ for the tails and between the tails and the headgroup $k_\theta = 6$ and $\theta_0 = 90°$. Two consecutive beads are connected by harmonic springs,

$$U_r = (1/2)k_r(r - r_0)^2, \quad (3)$$

with spring constant $k_r = 100$ and equilibrium distance $r_0 = 0.7$.

The model of the alcohols consists of one hydrophilic head bead and a tail that varies in length from one to three hydrophobic beads (see Fig. 2). Using the mapping procedure in which one DPD particle represents a volume of 90 Å^3, the alcohols methanol through pentanol correspond with the coarse-grained models ht and ht_2 and hexanol and heptanol corresponds with the model ht_3. The bond-bending potential with $k_\theta = 6.0$ and $\theta_0 = 180°$ was also applied between three consecutive beads of these alcohols.

A biological membrane is not subject to external constraints and therefore adopts a configuration which is tensionless. Lipowski and co-workers (Goetz and Lipowsky,

1998; Goetz et al., 1999) emphasize the importance of simulating at exactly the area for which the interfacial tension is zero and determine this area iteratively. We use a different approach in which we mimic the experiment by simulating an ensemble in which we impose the interfacial tension. After a randomly selected number of DPD steps we perform a Monte Carlo move in which we change the area of our bilayer in such a way that the total volume of the system remains constant. This move is accepted with a probability (Venturoli and Smit, 1999)

$$\mathrm{acc}(o \rightarrow n) = \min\left(1, \frac{\exp\{-\beta[U(n) - \gamma A_n]\}}{\exp\{-\beta[U(o) - \gamma A_o]\}}\right), \quad (4)$$

where $U(o)$ and $U(n)$ indicate the energy of the old and the new configuration, respectively, γ the interfacial tension, A the area of the bilayer, and $\beta = 1/k_B T$. To obtain the tensionless state, the bilayer is set to zero to ensure that the membrane adopts the equilibrium area per lipid (Kranenburg et al., 2003a,b). The importance of this method is that it allows us to observe directly phase transitions in which the area per lipid changes.

The system was initialized by placing 200 phospholipids and 20–200 model alcohols randomly in a simulation box. 3200–6700 water particles were added to ensure that a bilayer does not have any interaction with its periodic image. At a temperature of $T^* = 1.0$ a bilayer was formed, using DPD steps only. After the formation of the bilayer we allowed the bilayer to adopt a tensionless configuration by applying both DPD and Monte Carlo, in which the area of the bilayer is changed. We then slowly cooled the system from $T^* = 1.0$ to $T^* = 0.1$. A typical simulation required 100,000 cycles of which 20,000 cycles were needed for equilibration. Per cycle it is chosen with a probability of 70% whether to perform 50 DPD time steps or to make an attempt to change the area of the box. This equilibration time was set by monitoring the area per lipid at low temperatures. It takes relatively long before this property reaches a new equilibrium value once the temperature or the number of alcohols was changed. Since the bilayers are formed by self-assembly the leaflets of the bilayer can end up with a very different number of alcohols or lipids. If this difference was >10% we reinitialized the system until a membrane was obtained with a more equal distribution of alcohols and lipids over the two leaflets. To test the reproducibility of our simulations, we repeated the self-assembly from different initial condition and by heating of the system and subsequent cooling. Within the statistical uncertainty, these simulations with different initial conditions gave identical results. More details on the simulations can be found in Venturoli and Smit (1999) and Kranenburg et al. (2003b).

In our simulations we use the conventional reduced units, i.e., using r_c as the unit of length and $a = 1$ as the unit of energy. For some properties it is interesting to make a direct comparison with experiments. The conversion factor for the
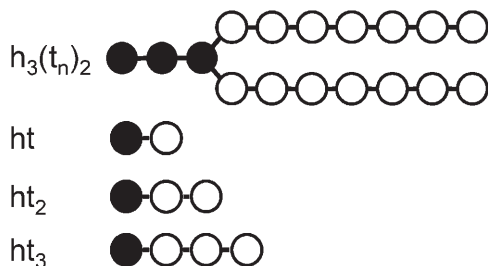

FIGURE 2   Models used in the simulations with their nomenclature. The letter n denotes the number of hydrophobic beads in the tails.

length scale from the assumption is that a DPD particle occupies a volume of 90 Å^3. For the temperature scale the conversion is less straightforward. The coarse-graining procedure of Groot can be used at any temperature; that is, if we are interested at higher temperature we can again match the compressibility and Flory-Huggins solubility parameters at the temperature of interest. This leads to temperature-dependent parameters that make the interpretation of the results more difficult. To avoid these difficulties we have used the experimental phase transition temperatures (without alcohol) to relate the DPD energy and temperature scales to the experimental system. With these parameters our simulations predict an area per surfactant of 69 Å^2 of the membrane in the L_α or fluid phase, independent of the chain length. This is in good agreement with the experimental values which are in the range 58–72 Å^2. For the area per lipid in the gel phase we find $A_l = 46.6$ Å^2, whereas the experimental value is $A_l = 47.2$ Å^2 (Tristram-Nagle et al., 2002).

RESULTS AND DISCUSSION

In this section we will focus on the phase diagram of the lipid $h_3(t_7)_2$ with different model alcohols as a function of temperature and the concentration of alcohol at the interface and we shortly describe the influence of changing the tail length of the lipid.

Phase behavior

In our simulations we observe that at high temperatures the bilayer is in the L_α phase. With decreasing temperatures, different phases are formed, depending on the concentration of alcohol in the bilayer (N_{alc}). In Fig. 3 snapshots are shown of the various low temperature phases of the lipid $h_3(t_7)_2$ at three concentrations of the model alcohol ht_2. At low alcohol concentrations (Fig. 3 a), we find the noninterdigitated (sub)gel phase L_c as the low temperature phase. The alcohols are homogeneously distributed at the interface, but the
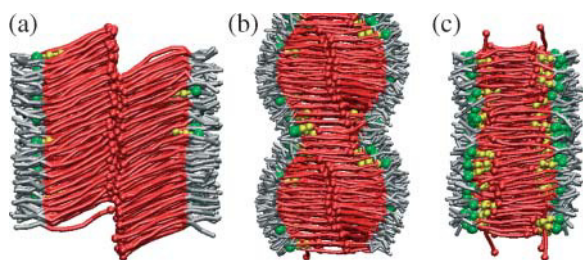

FIGURE 3 Snapshots of a bilayer consisting of the lipid $h_3(t_7)_2$ with various concentrations of the model alcohol ht_2 at $T^* = 0.25$. The bonds represent the lipids, with gray indicating the hydrophilic headgroups and red the hydrophobic tails. The yellow and green bonds and spheres representation indicates the alcohol molecules, where the green sphere is the hydrophilic headgroup. The terminal beads of both the lipid and the alcohol are depicted by a larger sphere. In b the system is depicted twice, so that the coexistence is illustrated more clearly.

concentration is too low to induce interdigitation. Experimentally, it is observed that in this region of the phase diagram the tilt angle of the lipid tails increases to a maximum of 50° (Nagel et al., 1992; Vierl et al., 1994) to compensate the additional space between the tails. We do not observe an increase in the tilt angle: the average tilt angle is constant (26°) with increasing number of alcohols from 0 to 30. In the L_α phase there is considerable lateral diffusion. In the gel phases the lateral diffusion is far less. At high alcohol concentrations the interdigitated gel $L_{\beta I}$ is formed, in which the lipid tails do not have a tilt with respect to the bilayer normal. The tails of the lipids of one monolayer are fully interpenetrated into the opposing layer and the tail ends are facing the tail end of the alcohol (see Fig. 3 c). In between these two extremes we find that there is coexistence between the interdigitated and noninterdigitated phases (Fig. 3 b). The alcohols are mainly located in the interdigitated part of the bilayer. To check the consistency of the results we repeated some simulations by heating the systems. We found that for these systems the equilibration from an interdigitated phase to the L_α phase took longer than the reverse path. The transition occurred at the same temperature, and no hysteresis was observed.

To study the influence of the tail length and concentration of alcohol in more detail, we calculated the phase diagrams of $h_3(t_7)_2$ with the model alcohols ht, ht_2, and ht_3. In Fig. 4 these phase diagrams are plotted as a function of temperature and the mole fraction of alcohol. To locate the phase boundaries we computed various order parameters to distinguish among the different phases: the area per lipid A_l, the extent of tail overlap D_c, and the ordering of the tails S_{tail}. By studying the behavior of these quantities as function of temperature and alcohol concentration we can determine the phase boundaries by determining the inflection point of the various order parameters. The transition from an ordered phase to a disordered one is very gradual. This gradual transition makes it difficult to determine the exact location of the phase boundaries, but the inflection point as our definition of the phase boundary gave consistent temperatures if we used, for example, as criterion the inflection point in A_l or in D_c for the location of the main transition. To investigate the effect of the system size we have repeated some simulations for much larger systems, which gave the same phase boundaries.

The phase diagrams nicely resemble the experimental phase diagram (see Fig. 1). The high-temperature phase in all cases is the L_α phase. The low-temperature phase is, dependent on alcohol concentration, the L_β phase, the $L_{\beta I}$ phase, or a coexistence between these two phases. We observe that the length of the alcohol molecule had little influence on the $L_{\beta I} \rightarrow L_\alpha$ transition, but the shorter the alcohol, the more stable the $L_{\beta I}$ phase. At lower temperatures the concentration of alcohol required to obtain the fully interdigitated phase increases, which is in agreement with the experimental observations of Nambi et al. (1988).
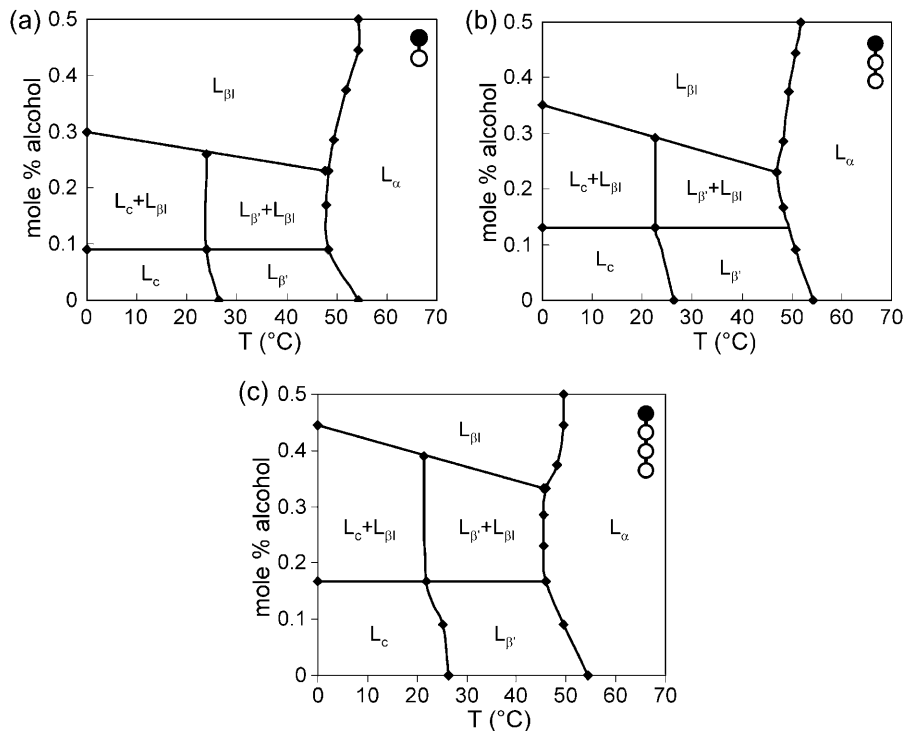
FIGURE 4 Phase diagrams of the lipid $h_3(t_7)_2$ with the model alcohols ht (a), ht_2 (b), and ht_3 (c). The dot at zero alcohol concentration indicates the transition from the gel phase $L_{\beta'}$ to the rippled phase $P_{\beta'}$, as was observed in Kranenburg et al. (2004b). For the definition of the various phases, see Fig. 1. The symbols are simulation results and the lines are a guide to the eye.

We also observe the biphasic effect on the main transition from the gel phases ($L_{\beta'}$, $L_{\beta'} + L_{\beta I}$, or $L_{\beta I}$) to the fluid L_{α} phase in our simulations: at a low mole fraction alcohol, the transition temperature shifts to a lower temperature. Increasing the number of alcohols leads to an increasing melting temperature. If interdigitation is complete, the melting temperature is almost constant. Comparing the different chain lengths of the alcohols shows that the transition from the fully interdigitated phase to the fluid phase slightly decreases with increasing chain length. Experimentally, this transition temperature is difficult to locate, since large hysteresis of this main transition was noted (Rosser et al., 1999; Tenchov et al., 1989; Rowe, 1985; Vierl et al., 1994). In a pure lipid bilayer, we observed the rippled phase $P_{\beta'}$ (Kranenburg et al., 2004b). Much larger systems are required than that studied in this work, to study the affect of alcohol in the stability of this phase. Therefore, we did not investigate this part of the phase diagram in detail.

Experimentally, a coexistence region between the non-interdigitated gel phase or the rippled phase and the interdigitated $L_{\beta I}$ is observed, if the concentration of alcohol is increased at a constant temperature (Vierl et al., 1994; Löbbecke and Cevc, 1995; Ohki et al., 1990). Nagel et al. (1992) observed the coexistence of the $L_{\beta'}$ and $L_{\beta I}$ phases in a DPPC/ethanol system. Mou et al. (1994) assume that this coexistence can occur due to an inhomogeneous distribution of the alcohol in the bilayer. If the ethanol molecules could aggregate to certain regions, the local ethanol concentration in certain areas is increased to above the critical value, so that a mosaic pattern of interdigitation can be formed. Even at

very low alcohol concentrations, very narrow domains of the interdigitated phase are formed (Mou et al., 1994). Our simulations confirm that the alcohol molecules are indeed inhomogeneously distributed in the lipid bilayer. We find that, at a constant temperature, in the observed coexistence region the mole fraction of alcohols in the interdigitated phase is constant. The mole fraction of alcohols in the noninterdigitated part increases with increasing number of alcohols. This explains the experimentally observed coexistence region: at a fixed temperature, the part of the bilayer that is interdigitated increases and the noninterdigitated part decreases with increasing alcohol concentration.

All experimental investigations study the interdigitation as a function of the concentration of alcohol in the bulk. The critical concentration at which interdigitation is complete ($c_{L_{\beta I}}$) decreases with increasing length of the alcohol (Löbbecke and Cevc, 1995; Rowe, 1983; Rowe and Campion, 1994). However, the concentration in bulk is not necessarily equal to the concentration of alcohol in the lipid bilayer. To relate the concentration of alcohol in bulk with the concentration of alcohol in the bilayer, the membrane buffer or partition coefficient K_p is often used. K_p describes the ratio of the solute concentration in the bulk water and in the lipid bilayer and its value increases with increasing chain length of the alcohol, caused by the hydrophobic effect (Rowe et al., 1998; Rowe and Campion, 1994; Connors, 1987). Experimentally, the distribution of alcohol between water and lipid vesicles can be determined and it is assumed that this distribution is equal to K_p in a lipid bilayer. There is little consensus in the literature whether this procedure yields

a reliable estimate of the alcohol concentration in the bilayer (Simon et al., 1977; Trandum and Westh, 2000; Trandum et al., 1999; Westh and Trandum, 1999; Westh et al., 2001). For example, it is assumed that the structure of the vesicle bilayer is representative for the bilayer phases; however, depending on the temperature, an alcohol molecule has a different affinity for the different phases in the order $L_{\beta I}$ (or L_α) $> L_\alpha$ (or $L_{\beta I}$) $> P_{\beta'} > L_{\beta'}$ (Rowe and Campion, 1994; Nambi et al., 1988; Löbbecke and Cevc, 1995; Zhang and Rowe, 1992), which is not taken into account.

Using computer simulations, we impose a number of alcohols in the bilayer. Comparing the phase diagrams of $h_3(t_7)_2$ with three different alcohols shows that there is little difference between the concentration of alcohols of ht and ht_2 needed to obtain the fully interdigitated phase $L_{\beta I}$, but that the concentration of the alcohol ht_3 is higher. We observe that for the alcohols ht_2 and ht_3 all alcohols are at the interface, independent of the number of alcohols. These results are in agreement with the conclusions of Rowe and Campion (1994). They found, using the bilayer partition coefficient, that for pentanol the concentration of alcohol in the bilayer is almost constant, but that for hexanol and heptanol, higher concentrations are needed. For the alcohol ht we observe that at the highest number used, some alcohols diffuse into the bulk water, forming micelles. This is consistent with the experimentally observed values of K_p, that indicates that adsorption of the alcohols at the interface is due to the hydrophobic effect.

Structure of the interdigitated phase

The structure of the interdigitated phase is still not well known. Adachi et al. (1995) proposed a model in which the terminal methyl group of the alcohol faces a terminal methyl group of a lipid chain (see Fig. 5). The assumption is based on the observation that the membrane thickness increases by ~0.08 nm per one methylene unit in both the alcohol molecules and the phospholipids. This distance of 0.1 nm is

the length of one CH_2-unit in the stretched chain of an alkane (Pauling, 1960). The small difference might be due to fluctuations in the hydrophobic chains. Furthermore, Adachi et al. (1995) show that two alcohol molecules can occupy a volume surrounded by the PC headgroups of one layer. From this it follows that the number of alcohol molecules should be twice as high as the number of lipids in the bilayer. Given the concentrations in the experimental procedure to determine the concentration at the interface, it is of interest to use simulations to investigate this interpretation of the experimental data in detail.

In our simulations we calculated the hydrophobic thickness D_c for combinations of the lipids $h_3(t_6)_2$ through $h_3(t_8)_2$ with the alcohols ht through ht_3 (see Fig. 6). The computed hydrophobic thickness D_c is for any combinations of lipids and alcohols in surprisingly good agreement with the experimental data considering the simplicity of the model. All combinations lead to a linear relation between D_c and the total number of beads. We compare this trend with half the hydrophobic thickness of a pure lipid bilayer, varying the tail length of the lipid from 5 to 8. For the pure bilayer we observe that the agreement of the simulated thickness and the experimental thickness becomes less satisfactory for the longer lipids. This could indicate that our mapping of three carbons in a tail onto one DPD bead may not be optimal. Alternatively, the data in Fig. 6 are for membranes in the L_β phase, which are stable at lower temperatures than the L_α for which the DPD parameters are optimized. Our model reproduces the chain length dependence of the L_α phase better. We observe that the slope of
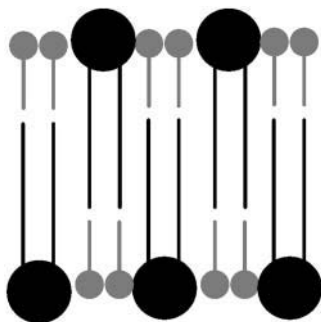
FIGURE 5 Proposed model of the interdigitated phase by alcohols (Adachi et al., 1995), in which every tail end of a phospholipid is facing the tail end of an alcohol. Solid molecules represent the phospholipids and shaded molecules the alcohols.
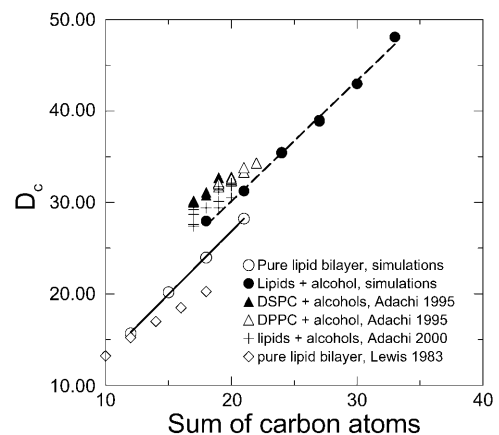
FIGURE 6 Comparison of the experimentally measured (Lewis and Engelman, 1983; Adachi et al., 1995; Adalsteinsson and Yu, 2000) and simulated thickness of the hydrophobic core D_c as a function of the total number of beads of the lipid and the alcohol. The length of alcohol tails ranges from one to three, and the length of the lipid tails from six to eight beads. The hydrophobic thickness of the pure lipid bilayer is divided by 2. All thicknesses are measured at a fully interdigitated bilayer, in which the ratio $N_{alc}/N_{lipid} = 1$:1. The lines are the best fits of the pure lipid system and the mixtures of lipids and alcohols. We only show the results for this ratio; similar results have been obtained for lower alcohol concentrations.

the best fits of these two data sets are almost the same, which is in agreement with the experimentally obtained results (Adachi et al., 1995; Adachi, 2000). Based on this dependence of the hydrophobic thickness on the total number of beads, Adachi et al. (1995) proposed the model depicted in Fig. 5, in which the alcohol/lipid ratio equals 2:1. However, our simulations show the same dependence, but at much lower concentrations. In Fig. 6, only the results for the ratio $N_{alc}/N_{lipid} = 1:1$ are given, but the same graph is obtained for lower alcohol concentrations, provided that the concentration is sufficient to induce the fully interdigitated $L_{\beta I}$ phase.

We observe that the fully interdigitated phase occurs at a much lower number of alcohol molecules in the bilayer than at twice the number of lipids. Interdigitation can be induced at much lower concentrations in the lipid bilayer than proposed in Adachi et al. (1995). This can be explained by taking into account an energy balance between the noninterdigitated and interdigitated phase. By the incorporation of alcohols at the membrane interface, voids are created in the hydrophobic core, which are energetically unfavorable (see Fig. 7, *left image*). The more alcohol, the higher the energy of the membrane. In the interdigitated phase the tail ends of the lipid are in contact with the interfacial water (see Fig. 7, *right image*). Adding alcohol reduces these energetically unfavorable interactions and hence increasing the alcohol concentration decreases the energy of the membrane. Clearly at the 2:1 ratio, the energy of the interdigitated phase will be lowest, but at much lower alcohol concentrations the energy can already be lower compared to the $L_{\beta'}$ phase.

To use this model quantitatively, one would need to take entropy effects into account as well, but this model does rationalize why we observe in our simulations already an interdigitated phase at much lower alcohol concentrations. For the model alcohol *ht*, our simulations show that the interdigitated phase is formed at a ratio alcohol/lipid $\approx$ 1:2, instead of 2:1 as proposed by Adachi et al. (1995). We also observed that the hydrophobic tail of the alcohol has rotationally more freedom than the lipid tails, meaning that

more than one phospholipid tail can be shielded from water by one alcohol molecule.

With this model, we can also understand the dependence on alcohol length of the stability of the $L_{\beta I}$ phase. The longer the alcohol, the smaller the voids in the alcohol-saturated $L_{\beta'}$ phase (see Fig. 8). The addition of a longer alcohol molecule perturbs the bilayer in the $L_{\beta'}$ phase to a lesser extent compared to a smaller one. For the interdigitated phase, however, Fig. 6 shows that a longer alcohol results in a thicker hydrophobic core. A void in this phase exposes, therefore, more hydrophobic groups of the lipids to the water phase compared to the shorter alcohols. These combined effects explain why the longer the tail length of the alcohol, the more alcohol is needed to stabilize the $L_{\beta I}$ phase. Similarly, we can understand why a higher concentration of alcohol is needed before the L_c phase is destabilized by a longer alcohol.

We also investigated the effect of increasing the chain length of the lipid. Experimentally, it was found that lower concentrations of alcohol are needed to obtain the fully interdigitated $L_{\beta I}$ phase (Rowe, 1983; Rowe and Cutrera, 1990; Nambi et al., 1988) and a coexistence region between an interdigitated and noninterdigitated phase was observed for most lipids (Vierl et al., 1994). There is no consensus in the literature whether a coexistence exists for the longest lipids. We performed simulations on bilayers consisting of $h_3(t_6)_2$ and $h_3(t_8)_2$ lipids, with alcohols varying in length from 1 to 3 beads in the tail. The obtained phase diagrams are similar to those depicted in Fig. 4. We find coexistence regions for each lipid-alcohol combination, which is in agreement with the results of Vierl et al. (1994). The size of the coexistence region decreases with increasing tail length of the phospholipid, because the concentration of alcohol to obtain the fully interdigitated phase decreases, whereas the alcohol concentration needed to destabilize the L_c and the $L_{\beta'}$ phase is independent of the alcohol concentration. The energy cost of exposing the tail ends to water becomes less important with increasing tail length, and therefore, the interdigitated phase is stabilized.
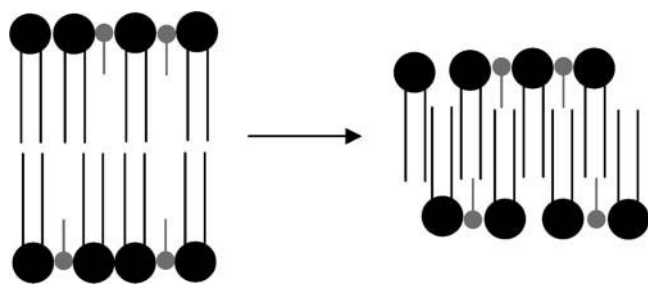

FIGURE 7 Schematic drawing of the formation of the interdigitated phase. Solid molecules represent the phospholipids and shaded molecules the alcohols. At a ratio lipid/alcohol $\approx$ 2:1, the interdigitated phase will be energetically more favorable than the noninterdigitated phase with voids between the hydrophobic tails, even if some of the tail ends are facing the interfacial water.
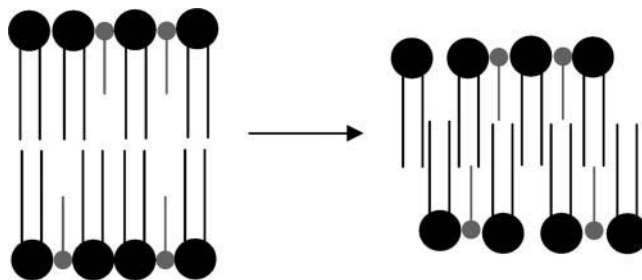

FIGURE 8 Schematic drawing of the formation of the interdigitated phase. With increasing tail length of the alcohol the voids become smaller in the $L_{\beta'}$ phase, whereas in the interdigitated phase the part of the lipid tails exposed to water becomes larger.

Longer chain alcohols

Experiments show that interdigitation only occurs in mixtures of lipids with alcohols up to heptanol. From octanol, therefore, longer chain lengths of the alcohol do not induce the interdigitated phase. The explanation of these observations is that the energy cost of creating lateral space in the headgroup region, leading to the formation of voids in the hydrophobic core, is balanced by the increased disorder in the lower part of the tails (Löbbecke and Cevc, 1995; McIntosh et al., 2001; Huang and McIntosh, 1997). We performed some simulations on the lipid $h_3(t_8)_2$ with the alcohols ht to ht_4. For alcohols ht to ht_3, we find similar phase diagrams to those shown in Fig. 4; increasing the length of the alcohol requires a higher alcohol concentration to stabilize the interdigitated phase. For ht_4, however, we do not find an interdigitated phase, but the structure shown in Fig. 9. In this structure we observe the coexistence of the L_c (or $L_{\beta'}$) phase with a new phase of which the hydrophobic thickness is approximately twice the hydrophobic length of the alcohol. In Kranenburg et al. (2003a,b), we have shown that single-tail lipids, which our model alcohol molecules resemble, can form a stable bilayer for sufficiently long tails. For these long-chain alcohols, the interdigitated phase has to compete with an alcohol-rich L_β or L_α phase.

Experimentally, it is observed that with the longer tail alcohols the $L_{\beta'}$ and the L_c are stabilized (Rowe and Campion, 1994). A phase separation, like we find in our simulations, is not observed. At this point, it is important to note that we did not optimize the parameters of our model to reproduce the properties of an alcohol: we used the same head and tail interactions as for our lipids and for the longer chain lengths these molecules resemble the single-tail lipids that are studied in Kranenburg et al. (2003a,b). In the literature, it is known that a mixture of two lipids does phase-separate in a lipid bilayer. The mixing of, for instance, lipids with different tail lengths, leads to the formation of domains
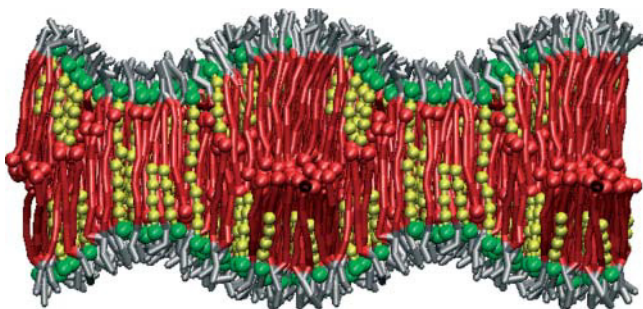
with the shorter lipid and domains containing the longer lipid (Risbo et al., 1995; Jorgensen et al., 1993). Since our model alcohols with tail lengths ≥ 4 self-assemble in a bilayer, our observations agree with the observations of a mixture of two bilayer lipids. Since we only investigated a small system, we cannot distinguish the formation of domains from an ordinary phase transition; it would be interesting to investigate this phase separation with larger systems.

CONCLUDING REMARKS

We studied the induced interdigitation of a bilayer consisting of double-tail lipids. In this work, interdigitation is induced by adding model alcohols to the bilayer. Using computer simulations, we can directly compute the concentration of alcohol in the lipid bilayer, which leads to an alternative approach of the formation of the interdigitated phase.

The main cause of the formation of the interdigitated $L_{\beta I}$ phase is an increase in the lateral area between the lipid headgroups. Due to this increase, voids are created in the hydrophobic core of the lipid bilayer. Since voids in the bilayer core are energetically unfavorable, the $L_{\beta'}$ or L_c phases are destabilized. These voids can be filled by molecules of the opposite monolayer. The bilayer will adapt an interdigitated configuration, in which the lipid tails of one monolayer interpenetrate the opposing layer. Increasing the repulsion between the lipid headgroups, increasing the lipid tail length, or decreasing the tail length of the alcohol, leads to an increase of the volume of these voids. The larger this volume, the more stable the interdigitated phase.

At low concentrations of alcohol the noninterdigitated gel phase is formed and at high concentrations the fully interdigitated phase is the stable phase. In between we find a coexistence region between the interdigitated and noninterdigitated phase, in which the alcohol molecules are inhomogeneously distributed between these two phases. We show that the interdigitated phase is formed at a lipid/alcohol ratio of $\sim$2:1, which is significantly lower than was proposed in the literature. At this ratio the formation of the interdigitated phase is energetically more favorable than a noninterdigitated structure with (energetically unfavorable) voids in the hydrophobic core, even if some of the lipid tail ends are exposed to the interfacial water.

FIGURE 9 Snapshot of a bilayer containing 200 lipids $h_3(t_8)_2$ and 200 alcohols ht_4. The bonds represent the lipids, with gray indicating the hydrophilic headgroups and red the hydrophobic tails. The yellow and green bonds and spheres representation indicates the alcohol molecules, where the green sphere is the hydrophilic headgroup. The terminal beads of both the lipid and the alcohol are depicted by a larger sphere. The system is depicted twice to show the phase separation more clearly.

REFERENCES

Adachi, T. 2000. A new method for determining the phase in the x-ray diffraction structure analysis of phosphatidylcholine/alcohol. *Chem. Phys. Lipids.* 107:93–97.

Adachi, T., H. Takahashi, K. Ohki, and I. Hatta. 1995. Interdigitated structure of phospholipid-alcohol systems studied by x-ray diffraction. *Biophys. J.* 68:1850–1855.

Adalsteinsson, T., and H. Yu. 2000. Lipid lateral diffusion in multi-bilayers, and in monolayers at the air/water and heptane/water interfaces. *Langmuir.* 16:9410–9413.

Chiou, J.-S., P. R. Krishna, H. Kamaya, and I. Ueda. 1992. Alcohols dehydrate lipid membranes: an infrared study on hydrogen bonding. *Biochim. Biophys. Acta.* 1110:225–233.

Connors, K. A. Binding Constants. John Wiley and Sons, NewYork,1987.

Feller, S. E., C. A. Brown, D. T. Nizza, and K. Gawrisch. 2002. Nuclear Overhauser enhancement spectroscopy cross-relaxation rates and ethanol distribution across membranes. *Biophys. J.* 82:1396–1404.

Frenkel, D., and B. Smit. 2002. Understanding Molecular Simula-tions: from Algorithms to Applications, 2nd Ed. Academic Press, London.

Furuike, S., V. G. Levadny, S. J. Li, and M. Yamazaki. 1999. Low pH induces an interdigitated gel to bilayer gel phase transition in dihexadecylphosphatidylcholine membrane. *Biophys. J.* 77:2015–2023.

Goetz, R., G. Gompper, and R. Lipowsky. 1999. Mobility and elasticity of self-assembled membranes. *Phys. Rev. Lett.* 82:221–224.

Goetz, R., and R. Lipowsky. 1998. Computer simulations of bilayer membranes: self-assembly and interfacial tension. *J. Chem. Phys.* 108: 7397–7409.

Groot, R. D., and K. L. Rabone. 2001. Mesoscopic simulation of cell membrane damage, morphology change and rupture by nonionic sur-factants. *Biophys. J.* 81:725–736.

Groot, R. D., and P. B. Warren. 1997. Dissipative particle dynamics: bridging the gap between atomistic and mesoscopic simulation. *J. Chem. Phys.* 107:4423–4435.

Hata, T., H. Matsuki, and S. Kaneshina. 2000. Effect of local anesthetics on the bilayer membrane of dipalmitoylphosphatidylcholine: interdigitation of lipid bilayer and vesicle-micelle transition. *Biophys. Chem.* 87:25–36.

Huang, C., and T. J. McIntosh. 1997. Probing the ethanol-induced chain interdigitations in gel-state bilayers of mixed chain phosphatidylcholines. *Biophys. J.* 72:2702–2709.

Jorgensen, K., M. Sperotto, O. G. Mouritsen, J. Ipsen, and M. Zuckermann. 1993. Phase-equilibria and local-structure in binary lipid bilayers. *Biochim. Biophys. Acta.* 115:135–145.

Koubi, L., L. Saiz, M. Tarek, D. Scharf, and M. L. Klein. 2003. Influence of anesthetic and nonimmobilizer molecules on the physical properties of a polyunsaturated lipid bilayer. *J. Phys. Chem. B.* 107:14500–14508.

Kranenburg, M., J.-P. Nicholas, and B. Smit. 2004a. Comparison of mesoscopic phospholipid-water models. *Phys. Chem. Chem. Phys.* 6:4142–4145.

Kranenburg, M., C. Laforge, and B. Smit. 2004b. Mesoscopic simulations of phase transitions in lipid bilayers. *Phys. Chem. Chem. Phys.* In Press.

Kranenburg, M., M. Venturoli, and B. Smit. 2003a. Molecular simulations of mesoscopic bilayer phases. *Phys. Rev. E.* 67:art. no. 060901.

Kranenburg, M., M. Venturoli, and B. Smit. 2003b. Phase behavior and induced interdigitation in bilayers studied with dissipative particle dynamics. *J. Phys. Chem. B.* 107:11491–11501.

Lewis, B. A., and D. M. Engelman. 1983. Lipid bilayer thickness varies linearly with acyl chain length in fluid phosphatidylcholine vesicles. *J. Mol. Biol.* 166:211–217.

Lewis, R. N. A. H., I. Winter, M. Kriechbaum, K. Lohner, and R. N. McElhaney. 2001. Studies of the structure and organization of cationic lipid bilayer membranes: calorimetric, spectroscopic, and x-ray diffrac-tion studies of linear saturated P-O-ethyl phosphatidylcholines. *Biophys. J.* 80:1329–1342.

Löbbecke, L., and G. Cevc. 1995. Effects of short-chain alcohols on the phase behavior and interdigitation of phosphatidylcholine bilayer membranes. *Biochim. Biophys. Acta.* 1237:59–69.

McIntosh, T. J., H. Lin, S. Li, and C.-H. Huang. 2001. The effect of ethanol on the phase transition temperature and the phase structure of monounsaturated phosphatidylcholines. *Biochim. Biophys. Acta.* 1510: 219–230.

McIntosh, T. J., R. V. McDaniel, and S. A. Simon. 1983. Induction of an interdigitated gel phase in fully hydrated phosphatidylcholine bilayers. *Biochim. Biophys. Acta.* 731:109–114.

Mou, J., J. Yang, C. Huang, and Z. Shao. 1994. Alcohol induces interdigitated domains in unilamellar phosphatidylcholine bilayers. *Biochemistry.* 33:9981–9985.

Nagel, N. E., G. Cevc, and S. Kirchner. 1992. The mechanism of the solute-induced chain interdigitation in phosphatidylcholine vesicles and characterization of the isothermal phase transitions by means of dynamic light scattering. *Biochim. Biophys. Acta.* 1111:263–269.

Nambi, P., E. S. Rowe, and T. J. McIntosh. 1988. Studies of the ethanol-induced interdigitated gel phase in phosphatidylcholines using the fluorophore 1,6-diphenyl-1,3,5-hexatriene. *Biochemistry.* 27:9175–9182.

Ohki, K., K. Tamura, and I. Hatta. 1990. Ethanol induces interdigitated gel phase ($l_{\beta i}$) between lamellar gel phase ($l_{\beta'}$) and ripple phase ($p_{\beta'}$) in phosphatidylcholine membranes: a scanning density meter study. *Biochim. Biophys. Acta.* 1028:215–222.

Pauling, L. 1960. The Nature of the Chemical Bond. Cornell University Press, New York.

Risbo, J., M. Sperotto, and O. Mouritsen. 1995. Theory of phase-equilibria and critical mixing points in binary lipid bilayers. *J. Phys. Chem.* 103:3643–3656.

Rosser, M. F. N., H. M. Lu, and P. Dea. 1999. Effects of alcohols on lipid bilayers with and without cholesterol: the dipalmitoylphosphatidylcho-line system. *Biophys. Chem.* 81:33–44.

Rowe, E. S. 1983. Lipid chain length and temperature dependence of ethanol-phosphatidylcholine interactions. *Biochemistry.* 22:3299–3305.

Rowe, E. S. 1985. Lipid chain length and temperature dependence of ethanol-phosphatidylcholines. *Biochim. Biophys. Acta.* 813:321–330.

Rowe, E. S., and J. M. Campion. 1994. Alcohol induction of interdigitation in distearoylphosphatidylcholine: fluorescence studies of alcohol chain length requirements. *Biophys. J.* 67:1888–1895.

Rowe, E. S., and T. A. Cutrera. 1990. Differential scanning calorimetric studies of ethanol interactions with distearoylphosphatidylcholine: transition to the interdigitated phase. *Biochemistry.* 29:10398–10404.

Rowe, E. S., F. Zhang, T. Wu Leung, J. S. Parr, and P. T. Guy. 1998. Thermodynamics of membrane partitioning for a series of *n*-alcohols determined by titration calorimetry: role of hydrophobic effects. *Biochemistry.* 371:2430–2440.

Shelley, J. C., M. Y. Shelley, R. C. Reeder, S. Bandyopadhyay, P. B. Moore, and M. L. Klein. 2001. Simulations of phospholipids using a coarse-grain model. *J. Phys. Chem. B.* 105:9785–9792.

Simon, S. A., and T. J. McIntosh. 1984. Interdigitated hydrocarbon chain packing causes the biphasic transition behavior in lipid/alcohol suspensions. *Biochim. Biophys. Acta.* 773:169–172.

Simon, S. A., W. L. Stone, and P. Busto-Latorre. 1977. A thermodynamic study of the partition of *n*-hexane into phosphatidylcholine and phosphatidylcholinecholesterol bilayers. *Biochim. Biophys. Acta.* 468: 378–388.

Slater, J. L., and C. H. Huang. 1988. Interdigitated bilayer membranes. *Prog. Lipid Res.* 27:325–359.

Tang, P., and Y. Xu. 2002. Large-scale molecular dynamics simulations of general anesthetic effects on the ion channel in the fully hydrated membrane: the implication of molecular mechanisms of general anesthesia. *Proc. Natl. Acad. Sci. USA.* 99:16035–16040.

Tenchov, B. G., H. Yao, and I. Hatta. 1989. Time-resolved x-ray diffraction and calorimetric studies at low scan rates. 1. Fully hydrated dipalmitoylphosphatidylcholine (DPPC) and DPPC/water/ethanol phases. *Biophys. J.* 56:757–768.

Trandum, C., and P. Westh. 2000. Alcohol-liposome interactions: a thermodynamic investigation. *Prog. Anesth. Mech.* 6:95–103.

Trandum, C., P. Westh, K. Jörgensen, and O. G. Mouritsen. 1999. A calorimetric investigation of the interaction of short chain alcohols with unilamellar DMPC liposomes. *J. Phys. Chem. B.* 103:4751–4756.

Tristram-Nagle, S., Y. Liu, J. Legleiter, and J. F. Nagle. 2002. Structure of gel phase DMPC determined by x-ray diffraction. *Biophys. J.* 83:3324–3335.

Veiro, J. A., P. Nambi, L. L. Herold, and E. S. Rowe. 1987. Effect of *n*-alcohols and glycerol on the pretransition of dipalmitoylphosphatidylcholine. *Biochim. Biophys. Acta.* 900:230–238.

Venturoli, M., and B. Smit. 1999. Simulating the self-assembly of model membranes. *Phys. Chem. Comm.* 2:art.no. 10.

Vierl, U., L. Löbbecke, N. Nagel, and G. Cevc. 1994. Solute effects on the colloidal and phase behavior of lipid bilayer membranes: ethanol-dipalmitoylphosphatidylcholine mixtures. *Biophys. J.* 67:1067–1079.

Westh, P., and C. Trandum. 1999. Thermodynamics of alcohol-lipid bilayer interactions: application of a binding model. *Biochim. Biophys. Acta.* 1421:261–272.

Westh, P., C. Trandum, and Y. Koga. 2001. Binding of small alcohols to a lipid bilayer membrane: does the partitioning coefficient express the net affinity? *Biophys. Chem.* 89:53–63.

Winter, I., G. Pabst, M. Rappolt, and K. Lohner. 2001. Refined structure of 1,2-diacyl-*p*-o-ethylphosphatidylcholine bilayer membranes. *Chem. Phys. Lipids.* 112:137–150.

Zhang, F., and E. S. Rowe. 1992. Titration calorimetric and differential scanning calorimetric studies of the interactions of *n*-butanol with several phases of dipalmitoylphosphatidylcholine. *Biochemistry.* 31:2005–2011.